J. Comp. Physiol. 141, 283–296 (1981)

Journal of Comparative Physiology · A

Analysis of the Cricket Auditory System by Acoustic Stimulation Using a Closed Sound Field*

Hans-Ulrich Kleindienst, Uwe T. Koch, and David W. Wohlers
Max-Planck-Institut für Verhaltensphysiologie, Abteilung Huber, D-8131 Seewiesen, Federal Republic of Germany

Accepted October 13, 1980

Summary. A closed sound field system for independent stimulation of both cricket hearing organs is described. The system was used to measure acoustic parameters of the peripheral auditory system in *Gryllus campestris* and to analyze inhibitory responses of the omega cell, a segmental auditory interneuron in the prothoracic ganglion.

1. Best sound transmission in the tracheal pathway occurs at 5 kHz. Closing of the prothoracic spiracles results in increased sound transmission but does not influence the frequency of best transmission in most animals (Fig. 6B). Sound transmission is modulated by abdominal contractions associated with the respiratory cycle (Fig. 7).

2. Attenuation Δ and phase shift φ in the tracheal pathway have been determined for the frequency range of 2 to 10 kHz in animals with closed spiracles. Δ shows a minimum at 5 kHz and φ increases almost linearly with frequency (Fig. 11).

3. Sound components acting on each side of the large tympanal membrane form a resultant sound pressure based on linear superposition. This resultant sound pressure represents the effective stimulus of the auditory sense organ (Fig. 12).

4. The response of the omega cell is dependent upon both intensity and relative phase of sound signals applied to the tympanal membranes (Fig. 10).

5. At 5 kHz, the response of the omega cell decreases linearly with increasing contralateral (inhibitory) stimulus intensity over a wide range of intensities. The latency between stimulus onset and response is nearly independent of contralateral inhibition (Figs. 15 and 16).

6. Response (spike number) differences between an omega cell and its complementary mirror image cell due to different stimulus intensities at both ears are enhanced by the neuronal mechanism of contralateral inhibition. In one animal the gain in spike number difference at 5 kHz was calculated to be 60% relative to the response difference when contralateral inhibition was disabled.

7. Evidence for a low frequency ($f \leqq 2$ kHz) ipsilateral inhibition of the omega cell is presented (Fig. 17).

* Supported by the Max-Planck-Gesellschaft

List of the Most Frequently Used Symbols

The subscript $i = 1,2$ of the following symbols refers to the respective sound cavity i of the closed sound field system.

M_i	= sound generating microphone in cavity i
T_i	= large tympanal membrane of the cricket leg in cavity i
TO_i	= tympanal organ of the cricket leg in cavity i
p_i	= sound pressure in cavity i
$\hat{p}_i$	= amplitude of p_i
L_i	= sound pressure level corresponding to p_i
p	= sound pressure acting on the internal side of tympanal membrane T_2
$\hat{p}$	= amplitude of p
Δ	= internal attenuation in the tracheal pathway
φ	= internal phase shift in the tracheal pathway
ΔL	= external attenuation used to compensate for Δ
$\Delta\varphi$	= external phase shift used to compensate for φ

Introduction

In the last two decades two aspects of the acoustic communication process in crickets, species-specific song recognition and directional hearing, have been widely investigated at many levels using a variety of experimental techniques.

Anatomically, the cricket peripheral hearing system includes an auditory organ located in the proximal part of each foreleg tibia. It is closely associated with the small leg trachea (Schwabe 1906; Michel 1974; Young and Ball 1974) which in turn communicates with the large leg trachea. The wall of the large trachea within the tibia is closely attached to the posterior tympanal membrane. This membrane is thought to be responsible for transmitting airborne sound to the tracheal system (Paton et al. 1977; Lar-

0340-7594/81/0141/0283/$02.80

sen and Michelsen 1978). The large leg tracheae are joined medially by a tracheal tube which has a thin medial septum; thus the two hearing organs are acoustically coupled. In addition, prothoracic spiracles, one on each side of the animal, also communicate external sound signals via this complex tracheal pathway to the hearing organs. Because of this peripheral construction, the cricket hearing system has become known as an H-shaped four-input system (Larsen and Michelsen 1978).

Recent studies on the cricket auditory system emphasize the biophysics of the ear with respect to tympanal membrane vibration (Johnstone et al. 1970; Paton et al. 1977; Larsen and Michelsen 1978), and consider the role of the tracheal system (Nocke 1974; Hill and Boyan 1976, 1977). Neuronal analysis includes the processing and distribution of directional information in the nervous system (Zhantiev et al. 1975a, b; Hill and Boyan 1976, 1977; Boyan 1978, 1979a, b) and effects of contralateral neuronal inhibition (Wohlers and Huber 1978; Wohlers 1980). The most complete theoretical analysis of the cricket hearing system is based on electrical networks (Fletcher and Thwaites 1979).

Until now most investigations have been made in free-field using a single sound source. When stimulating the four-input auditory system of the cricket under these conditions, changes of sound stimulus parameters will affect the sound field at each of the four inputs. Consequently, the contribution of any given input to the overall excitation of the auditory sense organs can be manipulated independently of the other ones only by moving the legs or blocking the corresponding tympanal membrane or prothoracic spiracle.

However, it may be advantageous to vary such stimulus parameters as time of onset, intensity, and phase relationship of one input to another when studying acoustical properties of the hearing system both biophysically and neuronally.

In this paper, we present a two-channel closed sound-field system with a frequency range of 0.3 to 20 kHz which produces sound pressure levels up to 95 dB[1] in cylindrical sound cavities. These cavities enclose the tibial parts of the cricket forelegs which are involved in sound reception. This results in the external isolation of each ear, simultaneously eliminating all problems with standing waves and effects of sound diffraction on the cricket body (Kleindienst 1978, 1980).

Using this closed-field system, the tracheal pathway within the peripheral hearing system is studied in detail. Further, responses of an acoustic interneuron, the omega cell, are shown and discussed relative to independent manipulations of the tracheal and nervous systems.

Materials and Methods

Theoretical Considerations and Cavity Design

A closed cylindrical box (which will be referred to as a cavity) of diameter d and length l has many acoustic resonance frequencies. For each frequency, a particular standing wave pattern can be observed. The lowest longitudinal resonance corresponds to a standing wave with only one maximum, and extends along the long axis of the cavity. This fundamental resonance frequency is given by $f=c/(2\cdot l)$ where c=sound velocity. Sound having a frequency lower than f cannot produce standing waves in the cavity. Therefore, we can measure the sound pressure in the cavity at one point and conclude that it is the same at all other points in the cavity, excluding a layer of about 0.4 mm from the walls of the chamber where the sound pressure is lower due to the viscosity of air. Cavities of this type are commonly used for calibrating microphones and for other precision acoustic measurements (Frederiksen 1977).

A cavity as shown in Fig. 1 was designed to stimulate the tympanal organ in crickets. It has an inside diameter of 6 mm and a length of 3 mm. We used a condenser microphone (Brüel and Kjaer, 1/4″, type 4135) as a sound source, the diaphragm of which formed the cavity's back wall. Two grooves for convenient insertion of the cricket leg were made in the side wall of the cavity. The front wall could be formed by either a control microphone (B and K, 1/4″, type 4136) or a simple brass cap producing the same inside dimensions, The theoretical value of the lowest resonance frequency in such a cavity is in the order of 56 kHz. Below this frequency the sound pressure in the cavity is proportional to the membrane deflection of the sound-transmitting microphone. This deflection is a square function of the voltage applied to the microphone terminals.

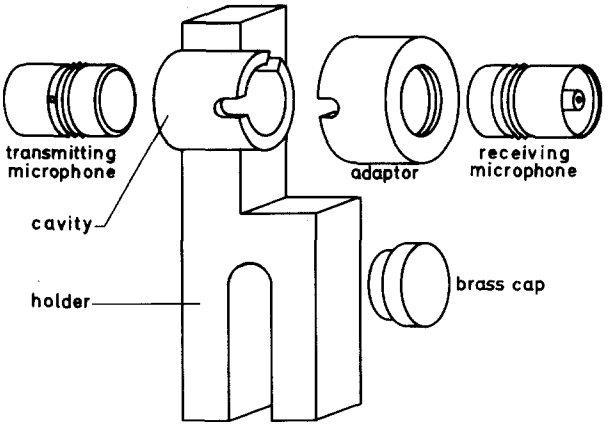

Fig. 1. The sound cavity used for closed sound field stimulation. The cavity consists of a short lucite tube which contains two grooves for insertion of the cricket leg. The transmitting condenser microphone produces the sound field in the cavity. The receiving microphone is used for control and calibration measurements. Normally this microphone is replaced by a brass cap which gives the same inside dimensions of the cavity

1 In this paper all sound pressure levels (SPL) are given in dB root mean square relative to $2\cdot 10^{-5}$ N/m^2

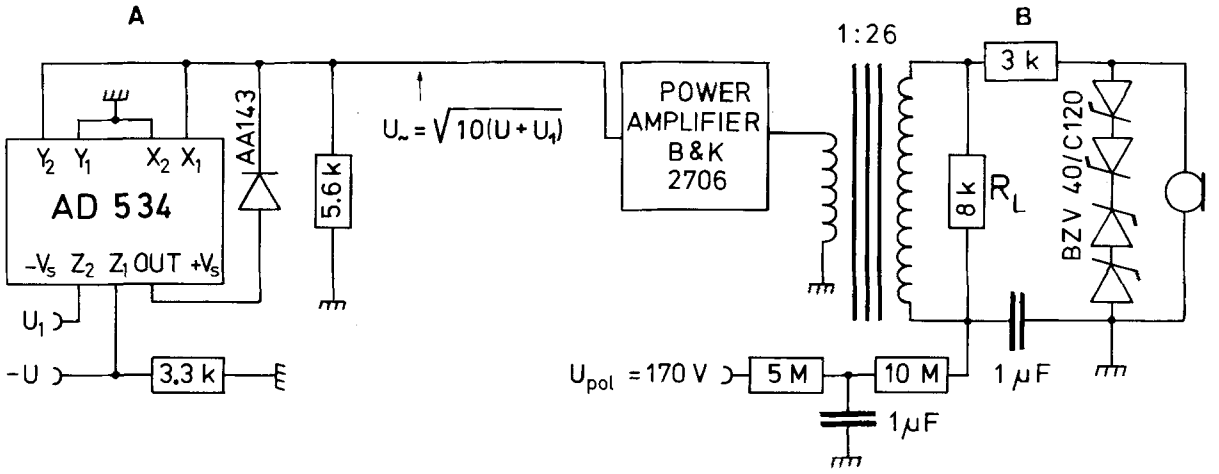

Fig. 2A, B. Distortion compensation and electrical connection of the condenser microphone used as a sound source. The voltage U representing the stimulus is predistorted by the square rooter (**A**) and coupled to the transmitting microphone (**B**) via a transformer. The load resistor R_L equalizes the frequency response of the transformer. The diode network 4 × BZV 40/C120 limits the output voltage to a safe level, thus preventing microphone damage

In our system this voltage consists of a constant DC polarization voltage U_{pol} and a superimposed alternating component $U_\sim$. When $U_\sim$ is a sinusoidal signal the square law of membrane deflection introduces strong harmonic distortions up to ca. 20%.

Principle of Distortion Compensation

The harmonic distortions caused by the square law were eliminated by introducing an inverse distortion to a sinusoidal voltage $U = \hat{U} \cdot \sin \omega t$. For this purpose, U was added to a constant voltage $U_1 \geqq \hat{U}$ to obtain positive values only. An IC precision multiplier (Analog Devices AD534) connected as a square rooter (Fig. 2A) then changes the signal to $U_\sim = \sqrt{10 \cdot (U + U_1)}$. A transformer adds the time-dependent Fourier components of $U_\sim$ to the polarization voltage U_{pol}; the resulting voltage is then coupled to the sound-transmitting microphone (Fig. 2B). With the peak voltage across the transmitting microphone at a safe level of 250 V, as much as 95 dB sound pressure can be reached. The quality of the distortion compensation was tested by measuring the total harmonic distortions with a B & K 1/4″ (type 4136) microphone connected to the sound cavity. Figure 3 shows a distortion factor below 1% in the region of main interest. The rise in the distortion factor to 3% above 15 kHz is due to the limited frequency band of the transformer used.

Stimulus Generation and Calibration

Figure 4 shows the complete stimulus setup as used in our experiments. To permit stimulation of both hearing organs, two cavities were provided and calibrated to the same output within 0.2 dB in the frequency range of main interest (1–10 kHz). Both channels are fed by the same sine generator; however, one of the channels can be given a defined phase lag $\Delta\varphi$ measured by a phase meter. The sine voltages in both channels are then transformed to sine wave pulses using two identical modulators and an envelope generator. The envelope generator signal thus controls pulse repetition rate, pulse duration, and ramp slope in both channels. Independent step attenuators set the gross sound pressure level in the cavities in 5 dB steps. An additional attenuator (ΔL), adjustable to 0.25 dB is included in the phase-lagged side. Attenuators, modulators, and the envelope-generating components (delay units, ramp generator) are building blocks of a multi-purpose stimulating system developed in the electronics workshop in Seewiesen.

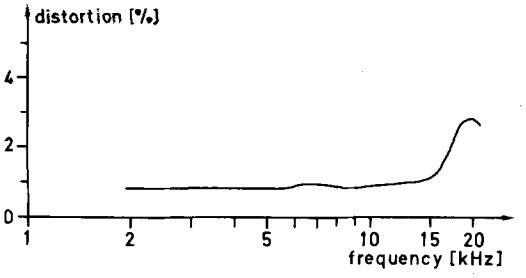

Fig. 3. Harmonic distortion in the closed sound field after distortion compensation. The distortion factor is less than 1% up to 15 kHz and remains below 3% in the total frequency range used

Figure 5 illustrates the acoustical properties of both channels with respect to frequency characteristics and the phase difference between the two sound cavities at a 95 dB setting. The calibration of absolute sound pressures had been made using continuous sine tones. For pulsed signals calibration was carried out by adjusting the pulse maximum to the same peak-to-peak amplitude of the continuous tones. This peak calibration gives a reliable value of maximum available sound pressure independent of instrument integration times or pulse duty cycles.

Animal Preparation and Neurophysiological Recordings

All experiments were done on female crickets (*Gryllus campestris* L.) four to ten weeks after adult molt. The animals were mounted ventral side up on a lucite sledge which could be adjusted within a dovetail guide supporting the sound cavities. The femura of the forelegs were horizontal and at right angles to the body axis. The tibial-femur angle was approximately 120°. In this position, the forelegs were fixed to the grooves of the sound cavities with insect wax. The 1/4″ microphones were then mounted and the brass caps waxed to the cavities. To test for leaks in the system, a 2 kHz sound generating probe (orifice diameter 0.4 mm) was moved around the external surface of the cavities and responses of the 1/4″ microphones were monitored. This test was important since even small leaks may change the calibration of the cavities and transmit external sound into the sound chambers. The same procedure was carried out after the prothoracic spiracles were

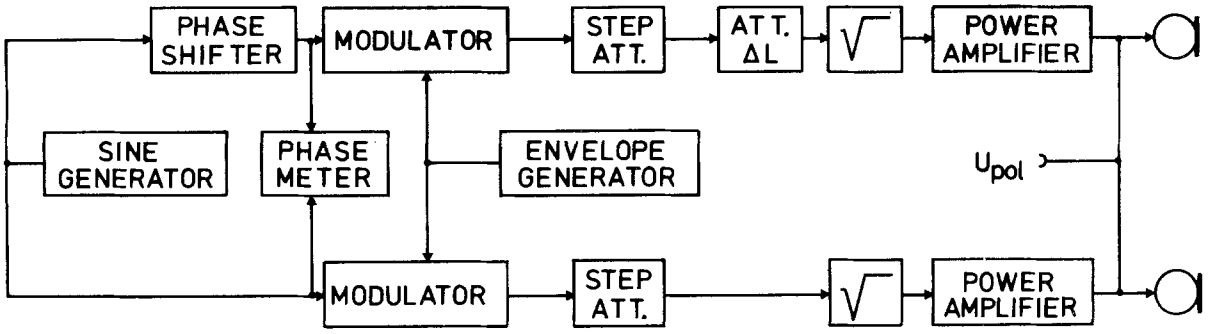

Fig. 4. Diagram of the sound generating equipment. Both channels are identical except for the phase shifter and attenuator ΔL in the upper channel. These additional components allow independent fine adjustment of relative intensity and phase between the two channels

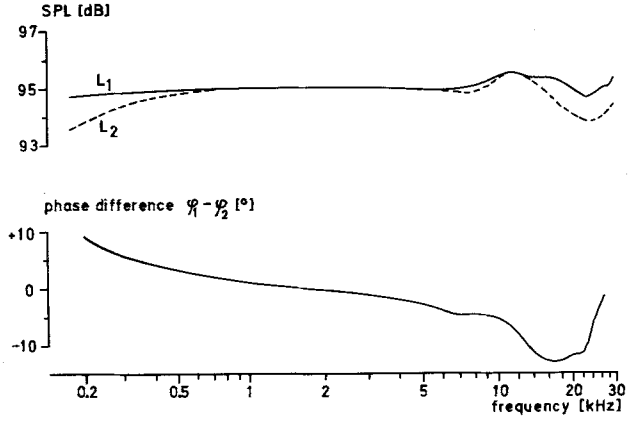

Fig. 5. Frequency and phase response of the closed-field stimulation system. Upper graph: sound pressure level in cavity 1 (solid curve) and cavity 2 (broken curve) for an intensity setting of 95 dB. Lower graph: phase difference $\varphi_1 - \varphi_2$ between the sound pressures in cavities 1 and 2

waxed over (see Results). All recordings of nervous activity were made intracellularly using glass microelectrodes (40–60 MOhm) filled with 3 M potassium acetate. Spike activity was stored on a Racal Store 4D tape recorder and simultaneously observed on-line by a digital counter.

Results

A. Biophysics of the Peripheral Hearing System

I. Sound Transmission Within the Tracheal System

Figure 6A illustrates the arrangement used to measure sound transmission from one side of the animal to the other via the tracheal pathway. The transmitting microphone M_1 produces a sound pressure $p_1 = \hat{p}_1 \cdot \sin \omega t$ in cavity 1 corresponding to a sound pressure level of 95 dB. p_1 acts on the external surface of the large tympanal membrane T_1. Sound travels through the main leg trachea to the other side, resulting in an unknown sound pressure $p = \hat{p} \cdot \sin(\omega t - \varphi)$ acting on the inner surface of tympanal membrane T_2. The motion of this membrane produces a sound pressure p_2 in cavity 2, the SPL L_2 of which can be measured by the receiving microphone M_2. A 1/3 octave filter (Wandel and Goltermann TB-1) reduces the influence of inherent noise from M_2 and its preamplifier on the measurement.

For a single animal, L_2 (corrected for the remaining 1/3 octave noise) is plotted versus frequency (Fig. 6B). Transmission with open spiracles shows a distinct optimum at 4.5 kHz (curve ●—●). After exposing the prothoracic ganglion for recording, a slight increase of transmission was observed (curve △—△). Since the state of the spiracles may influence hearing processes, transmission was also measured after the spiracles were waxed over (curve ○—○). The transmitted sound energy increased after removal of the spiracular 'leaks' in the system, but the frequency of best transmission did not change significantly.

The distribution of the frequency for best sound transmission in 24 animals is plotted in Fig. 6C, and shows a maximum at 5 kHz. In four animals no transmission could be measured in the frequency range used, and in three animals the transmission optimum decreased by 1.5 to 1.85 kHz after covering the spiracles with wax. All the other animals showed no significant frequency shift.

In intact animals sound transmission through the tracheal system may be influenced by respiration and movements of the animal. Figure 7 illustrates the modulating effect of abdominal contractions on sound transmission at 2.5 kHz for animals with closed spiracles. Here sound transmission was reduced by as much as 4 dB during contraction. This effect disappeared when the animal was opened to expose the prothoracic ganglion. Reduction of the transmitted sound could be produced by pinching the sound-guiding trachea. But almost complete compression of the trachea was necessary to produce an appreciable attenuation. At the frequency of optimal sound transmission, however, the region of the septum was ex-

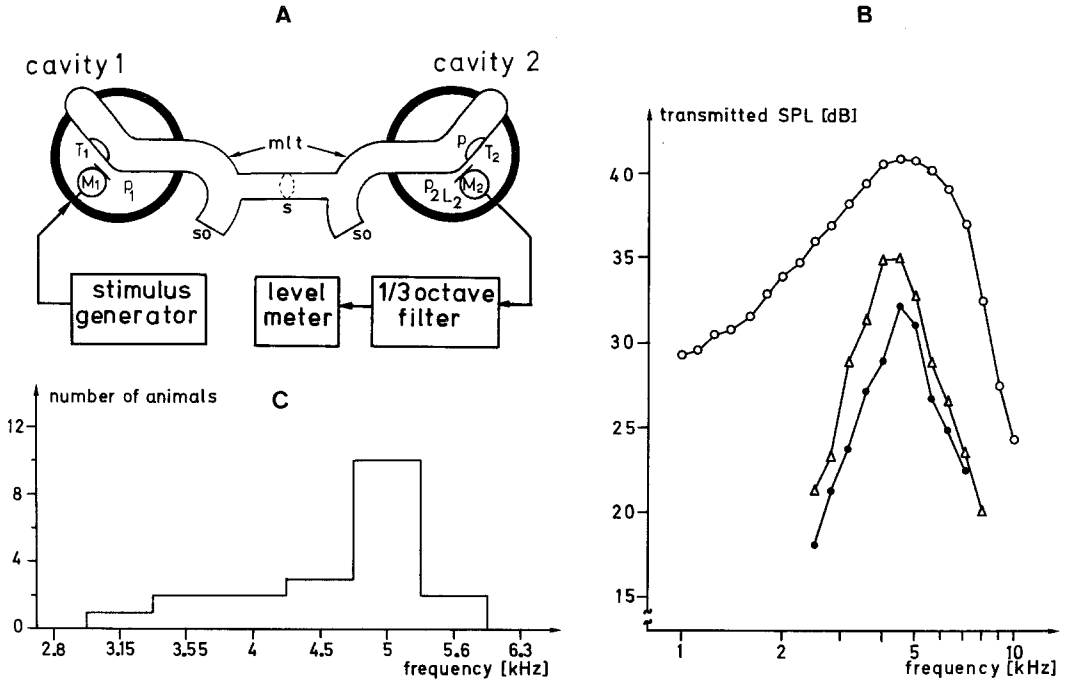

Fig. 6A–C. Sound transmission in the tracheal pathway. **A** Diagram of experimental arrangement. The sound transmitting microphone M_1 produces the sound pressure p_1 in cavity 1. Tympanal membrane T_1 transmits sound to the main leg tracheae (*mlt*). The spiracular openings (*so*) may be open or closed. Sound which passes the medial septum (*s*) produces the internal sound pressure p which acts on the inner surface of tympanal membrane T_2. Vibration of this membrane elicits sound pressure p_2 in cavity 2. The sound pressure level L_2 corresponding to p_2 is measured by microphone M_2. **B** Transmitted sound pressure level L_2 in cavity 2 for a constant 95 dB continuous tone stimulus in cavity 1. ●——● before, and △——△ after exposing the prothoracic ganglion for recording. ○——○ sound transmission after closing the spiracular openings with wax. **C** Distribution of the frequency for best sound transmission in 24 animals. In 4 animals no sound transmission could be measured

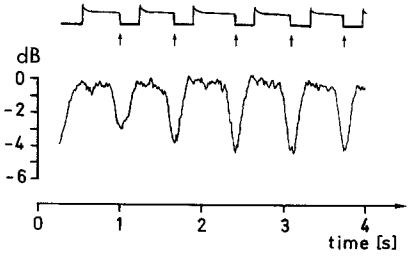

Fig. 7. Changes of sound transmission during abdominal contractions related to respiratory movements. Upper trace: recording of abdominal contractions (arrows indicate the peak of contraction). Lower trace: change of transmitted sound pressure, shown in dB

tremely sensitive to compression. Sound transmission was increased by 6 ± 2 dB in the frequency range of 4 to 8 kHz after the tympanal membrane and the tracheal wall associated with it were removed on the sound input side. After severing the main trachea near the septum, sound transmission was totally abolished.

II. Sound Attenuation Δ and Phase Shift φ in the Tracheal Pathway

The attenuation of the internal sound pressure p relative to p_1 in cavity 1 (see Fig. 6A) is defined by $\Delta = 20 \cdot \log(\hat{p}/\hat{p}_1)$ where $\hat{p}$ and $\hat{p}_1$ are the amplitudes of the respective sound pressures. (No emphasis was placed on the sign of the log-function.) To describe the internal coupling of both tympana, Δ rather than the amplitude $\hat{p}$ will be used. A direct measurement of Δ by insertion of a probe microphone into the trachea is difficult because of its small diameter (0.3 mm). Figure 8A shows how the arrangement of Fig. 6A was modified to enable an indirect measurement of Δ. Sound pulses of 20 ms duration and 2 ms rise and fall times were introduced into cavities 1 and 2 alternately. At a given sound frequency, the response of an omega cell, an acoustic interneuron in the prothoracic ganglion, was recorded for various intensities. This cell has its excitatory input exclusively on one side (e.g. tympanal organ TO_2 in Fig. 8A; see also Wohlers 1980). The spiracles were closed with wax to ensure a constant condition throughout the experiment. In Fig. 8B the response of an omega cell to a stimulus composed of 6 sound pulses, presented at a rate of 2/s and a sound frequency of 5 kHz, is plotted as total number of spikes versus intensity. The intensity difference between ipsilateral (curve ○——○) and contralateral (curve △——△) stimulation eliciting the same total number of spikes (20)

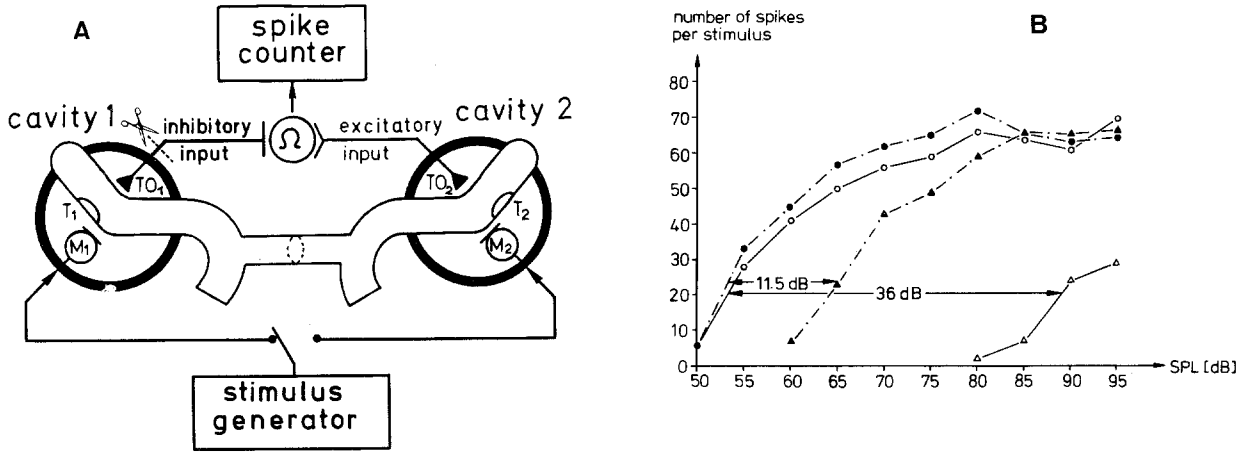

Fig. 8A, B. Intensity responses of an omega cell stimulated with 5 kHz sound signals. **A** Experimental arrangement. The spike counter measures the activity of the omega cell receiving excitatory input from tympanal organ TO_2 and inhibitory input from TO_1. **B** Intensity responses for various stimulus situations. Open symbols before, and closed symbols after elimination of the inhibitory input by severing the contralateral leg nerve. ●, ○ sound stimulus to the ipsilateral side (cavity 2). ▲, △ sound stimulus to the contralateral side (cavity 1)

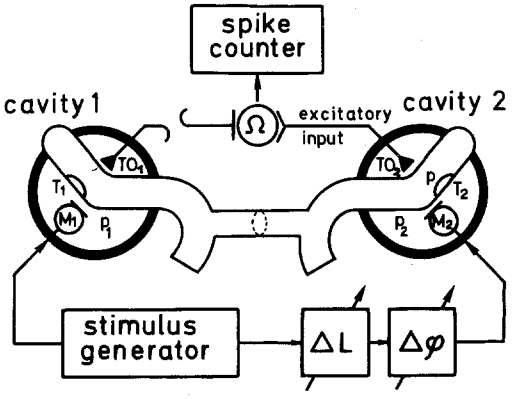

Fig. 9. Experimental arrangement used for cancelling experiments (further explanation in the text)

amounts to 36 dB. As the omega cell is known to be inhibited by sound stimulation from the contralateral side (Wohlers and Huber 1978; Wohlers 1980), this intensity difference is not only caused by the attenuation of the tracheal pathway, but also reflects the contralateral neuronal inhibition. Therefore, the experiment described above was repeated with the contralateral leg nerve cut (Fig. 8B, curves ●–·–● and ▲–·–▲), thus eliminating the inhibitory input to the recorded omega cell. Here the ipsi-contralateral intensity difference (equivalent to Δ) is reduced from 36 dB to 11.5 dB.

To determine the phase lag φ of the internal sound pressure p relative to p_1 in cavity 1 a phase shifter ($\Delta\varphi$) and an attenuator (ΔL) were added to the experimental setup (Fig. 9). Assuming that the tympanal organ TO_2 is excited by the vibration of tympanum T_2, the response of the omega cell reflects the strength of the resultant force driving T_2. If A denotes the area of the tympanal membrane T_2, then this force is given by $F=A\cdot(p_2-p)$. When the external attenuation ΔL is set to the internal attenuation Δ and the external phase shift $\Delta\varphi$ matches the internal phase shift φ then the driving force F becomes 0. In this situation, no sound energy is transferred to the tympanal organ TO_2 and the omega cell response should disappear. Experimentally, the contralateral sound pressure level L_1 in cavity 1 was set to 85 dB and a ΔL of 11.5 dB (equal to the value of Δ taken from Fig. 8B) was used. Thus a sound pressure level of 73.5 dB was established in cavity 2. The spiracles were closed and the contralateral leg nerve was cut. Under these conditions, Fig. 10A shows the response of the omega cell (number of spikes/6 pulses) plotted against the external phase shift $\Delta\varphi$ at 5 kHz.

There is a small gap δ between the two branches of the response curve. Within this gap the sound pressure difference p_2-p driving the tympanal membrane T_2 is not sufficient for supra-threshold excitation of the omega cell at 5 kHz. The internal phase shift φ can then be approximated by taking the value of $\Delta\varphi$ which corresponds to the center of the gap. For large gaps the accuracy of φ is determined by half the width of the gap, whereas for small gaps the accuracy of the phase meter ($\pm 1°$) is the limiting factor. From the data in Fig. 10A, $\varphi=156\pm 1$ degree.

Finally, after adjusting $\Delta\varphi$ to φ, the internal attenuation (of the tracheal pathway) can be more accurately determined by varying the external attenuation ΔL (Fig. 10B curve ●——●). Again the parameter of interest (Δ) is determined from the center of the gap; it is 11.3 ± 0.3 dB, confirming the previous value of Δ derived from the intensity characteristics

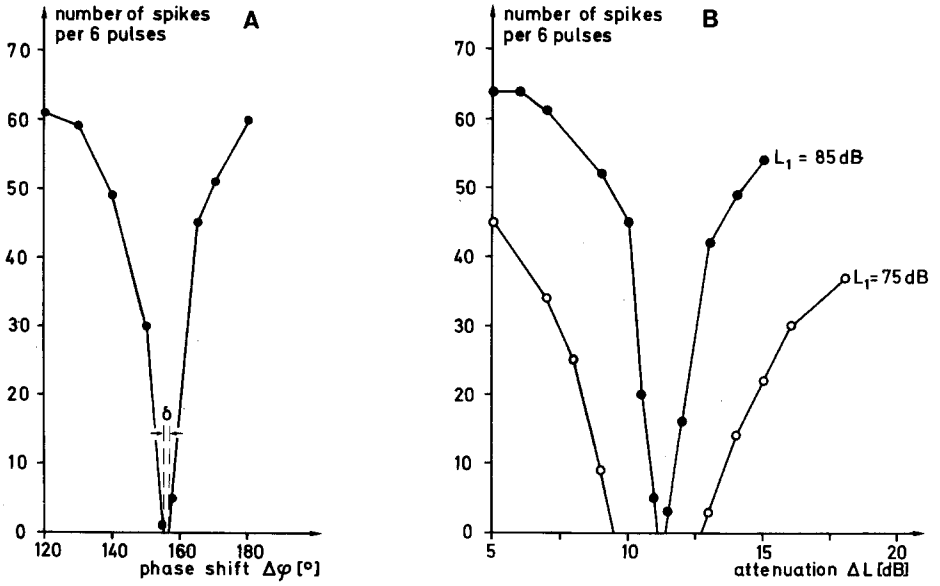

Fig. 10A, B. Response of an omega cell to simultaneously-presented ipsi- and contralateral sound stimuli at 5 kHz in the absence of contralateral inhibition (the contralateral leg nerve was severed). **A** Responses to various external phase shift $\Delta\varphi$. Sound pressure parameters: 85 dB SPL in cavity 1, external attenuation $\Delta L = 11.5$ dB; 73.5 dB SPL in cavity 2. **B** Dependence of the spike response upon the external attenuation ΔL at a constant external phase shift $\Delta\varphi$ of 156°. The intensity in cavity 1 was 85 dB (curve ●——●) and 75 dB (curve ○——○)

(Fig. 8B). Here the accuracy of Δ for small gaps is determined by the accuracy of the external attenuator ΔL (± 0.25 dB). The influence of the (arbitrary) sound pressure level L_1 in cavity 1 on the gap width δ becomes apparent from curve ○——○ in Fig. 10B taken at $L_1 = 75$ dB. High sound pressure levels must be used if the center value of the gap is to be determined accurately.

III. Frequency Dependence of Δ and φ

The methods described in detail for 5 kHz were used to determine Δ and φ in the frequency range of 2 to 10 kHz. The results are summarized in Fig. 11. Above 13 kHz sound energy transmitted by the trachea was not sufficient for supra-threshold excitation of the recorded omega neuron. The values of Δ obtained from the intensity characteristics (closed circles) and those from interference plots (open circles) match (Fig. 11A). Principally, the frequency dependence of Δ reflects the course of the transmission curve (Fig. 6B). The frequency of lowest attenuation is closely related to the frequency of best transmission. The internal phase shift φ is almost a linear function of frequency in the range investigated, indicating that prominent resonances do not occur in the system (Fig. 11B).

IV. Cancelling Experiments and Linear Superposition Hypothesis

Results reported so far, especially those from the cancelling experiment involving variable external phase

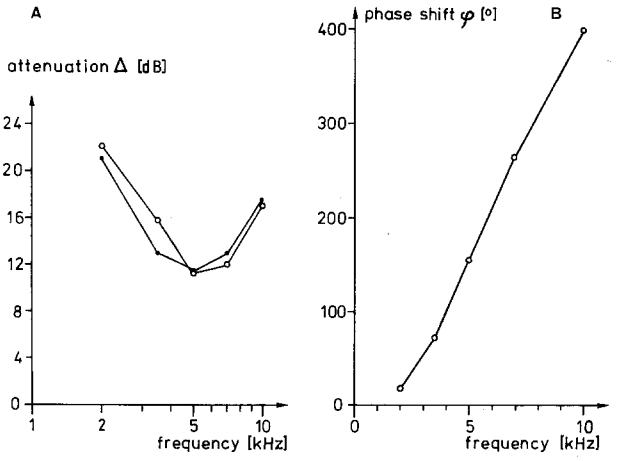

Fig. 11. A Frequency dependence of attenuation Δ and **B** internal phase shift φ in the tracheal pathway. In **A**, the attenuation is obtained from intensity/response characteristics (●——●) and from cancelling experiments (○——○)

lag $\Delta\varphi$, show conclusively that a combination of external and internal sound components produces a resultant force which acts upon the hearing organ.

Now we examine the extent to which a linear superposition hypothesis is reflected in the interaction of ipsilateral and contralateral sound within the cricket hearing system.

With the external phase shift $\Delta\varphi$ set to give optimum destructive interference, the resultant sound pressure level (L_{cal}) can be calculated on the basis of linear superposition of internal sound pressure p

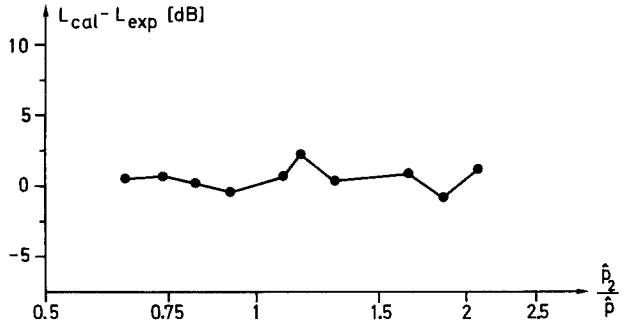

Fig. 12. Difference between the theoretical resultant sound pressure level L_{cal} (calculated on the basis of linear superposition between internal and external sound components) and experimental sound pressure level L_{exp}, plotted against the ratio of external ($\hat{p}_2$) and internal ($\hat{p}$) sound pressure amplitude

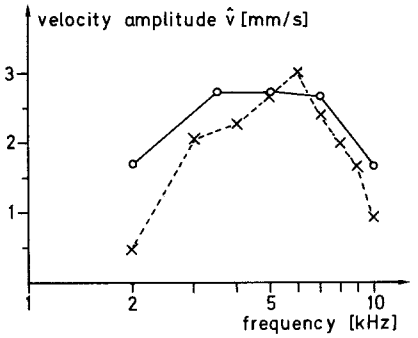

Fig. 13. Tympanal membrane vibration velocity extrapolated to a driving sound pressure level of 100 dB. o——o values obtained from sound transmission data in Fig. 6 B. x----x vibration velocity amplitude measured by laser vibrometry (redrawn from Fig. 5 in Larsen and Michelsen 1978; the high frequency data points were not considered)

Table 1. Internal attenuation Δ and phase shift φ of the tracheal pathway at 5 kHz measured in 8 different animals

Animal	State of spiracles	Δ (dB)	φ (°)
1	Untreated	11.8	25
2	Untreated	9	70
3	Untreated	11.8	68
4	Untreated	16.5	95
5	Untreated	17.5	80
5	Closed	11.3	156
6	Closed	14	153
7	Closed	14	134
8	Closed	8.5	155

and external sound pressure p_2. In the cancelling experiment (Fig. 10 B), the response of a given omega cell can be converted from spike number per stimulus to absolute intensity level (L_{exp}) using the response/intensity characteristic of that same cell (Fig. 8 B curve ●–●–●). For 5 kHz the difference $L_{cal} - L_{exp}$ between calculated and experimental resultant sound pressure level is displayed in Fig. 12 as a function of the ratio $\hat{p}_2/\hat{p}$ between external and internal sound pressure amplitudes. The scatter of $L_{cal} - L_{exp}$ around zero shows that the results of the cancelling experiment fully agree with the theoretical linear superposition hypothesis.

V. The Effect of the Spiracles

Table 1 summarizes attenuation Δ and phase shift φ data from different animals at 5 kHz for both untreated and experimentally closed spiracles. For animal 5, the reduction of attenuation Δ after closing the spiracles is found to be 6.2 dB (Δ untreated − Δ closed). This difference corresponds, in order of magnitude, to the increase of transmission at 5 kHz (see Fig. 6 B) in the same animal following the occlusion of the spiracles. When comparing the dependence of phase shift φ on the state of the spiracles (using animals from Table 1) one sees that closing of the spiracles yields an additional average phase shift of 70–80 degrees. This suggests that the animal may adjust the internal phase shift φ by partly closing the spiracles to give an optimal bilateral interaction.

At the present stage further conclusions about directional hearing in crickets can not be drawn since attenuation and phase shift contributions of the spiracular pathway have not yet been determined relative to the momentary state of the spiracles (for an estimation of the sound amplitude reaching the inner surface of the tympanum via spiracles see Larsen and Michelsen 1978).

VI. Tympanal Membrane Vibration Velocity

With the results of Fig. 11 A (sound attenuation Δ in the tracheal pathway) one can determine the amplitude $\hat{v}$ of the tympanal membrane vibration velocity using sound transmission data from the same animal (Fig. 6 B curve o——o). The mathematical procedure is described in Appendix A.

Figure 13, curve o——o, shows $\hat{v}$ extrapolated to a 100 dB level of the driving (internal) sound pressure p (cf. Fig. 6 A). The results are similar to those obtained from laser vibrometry on the same species (curve x----x, redrawn from Fig. 5 in Larsen and Michelsen 1978).

B. Physiology of the Omega Cell

I. Threshold Determination

The threshold sound pressure level L_t of the omega cell can be obtained from the cancelling experiments where the internal phase shift φ has been compensated by the external phase shift $\Delta\varphi$ (Fig. 10 B). At the boundaries of the gap δ, the difference $|p_2 - p|$ be-

tween external and internal sound pressure becomes equal to that required for a threshold response. For example, from curve o——o in Fig. 10B corresponding to $L_1 = 75$ dB one finds a threshold response at $L_2 = L_1 - \Delta L = 65.5$ dB and at $L_2 = 62.25$ dB, corresponding to a sound pressure (root mean square) $p_2 = 3.8 \cdot 10^{-2}$ N/m^2 and $p_2 = 2.6 \cdot 10^{-2}$ N/m^2, respectively. From the center of the gap one obtains the internal sound pressure (root mean square) $p = 0.5 \cdot (2.6 + 3.8) \cdot 10^{-2}$ N/m^2 $= 3.2 \cdot 10^{-2}$ N/m^2. Thus, the resultant sound pressure at the boundaries of the gap becomes $|p_2 - p| = 0.6 \cdot 10^{-2}$ N/m^2 and the threshold level at 5 kHz is $L_t = 49.5$ dB.

Further, independent of this method, L_t was measured directly on the same animal using closed sound-field stimulation on the input of the recorded omega cell. Here L_t was defined by a response of 1 to 3 spikes per 6 sound pulses. Figure 14 shows L_t derived both from cancelling experiments (curve +——+), and by direct measurement (curve o——o); the two curves match. A comparison of the threshold curve of an omega cell under closed-field conditions with a free-field threshold curve of an omega cell (curve ●——●, redrawn from Fig. 6A in Wohlers and Huber 1978) leads to the suggestion that minor oscillations in free-field threshold curves may be due to inhomogeneities of the sound field, diffraction and reflection of sound on the cricket body, and interaction between different sound components in the four-input system, effects which are eliminated when using the closed-field stimulus system.

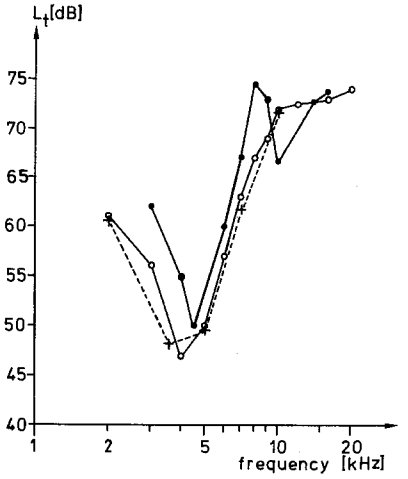

Fig. 14. Auditory threshold curves in open and closed sound fields. o——o Threshold curve of an omega cell measured in our closed sound field. +——+ Threshold curve of the same cell calculated from the cancelling experiments. ●——● Open-field threshold curve of an omega cell (redrawn from Fig. 6A in Wohlers and Huber 1978)

II. Inhibitory Inputs to the Omega Cell

The prothoracic ganglion of crickets contains a pair of complementary omega cells which mutually inhibit one another (Wohlers 1980). In order to study the inhibition, the 'legphones' were used to isolate the sound inputs (Fig. 15A). To prevent interaction between the tympana via the tracheal system, the tube

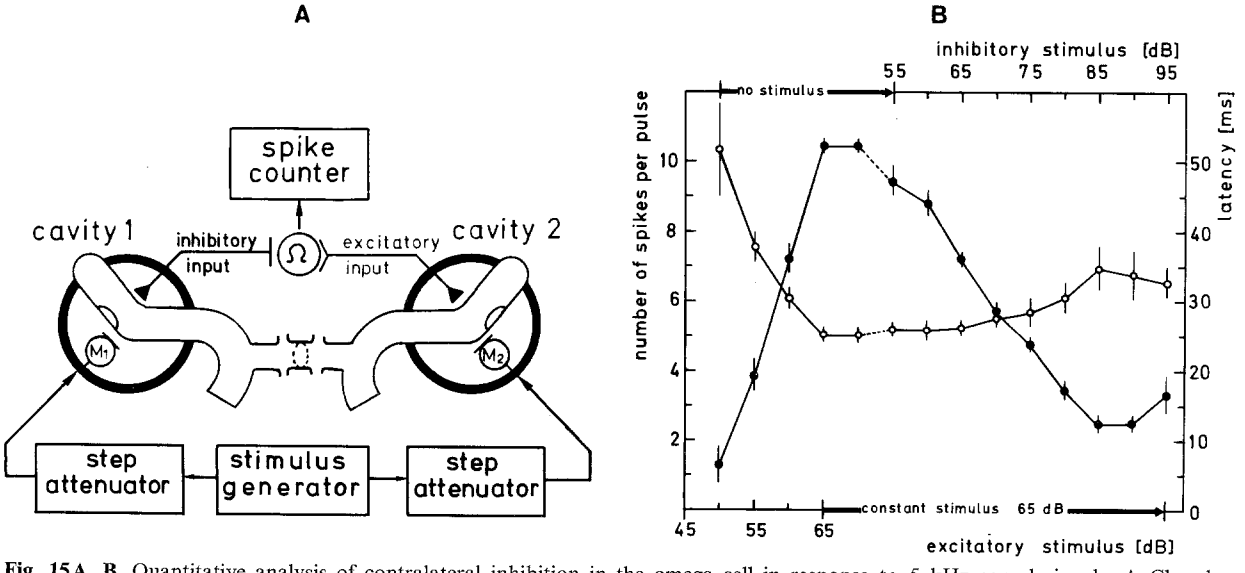

Fig. 15A, B. Quantitative analysis of contralateral inhibition in the omega cell in response to 5 kHz sound signals. **A** Closed sound field arrangement for external and internal isolation of excitatory and inhibitory inputs to the omega cell. **B** Response characteristic (●——●) and latency (o——o) of an omega cell for various excitatory and inhibitory stimulus settings. Symbols represent means of 30 consecutive sound presentations with standard deviations. Sound pulse duration: 50 ms, rise and fall times: 2 ms

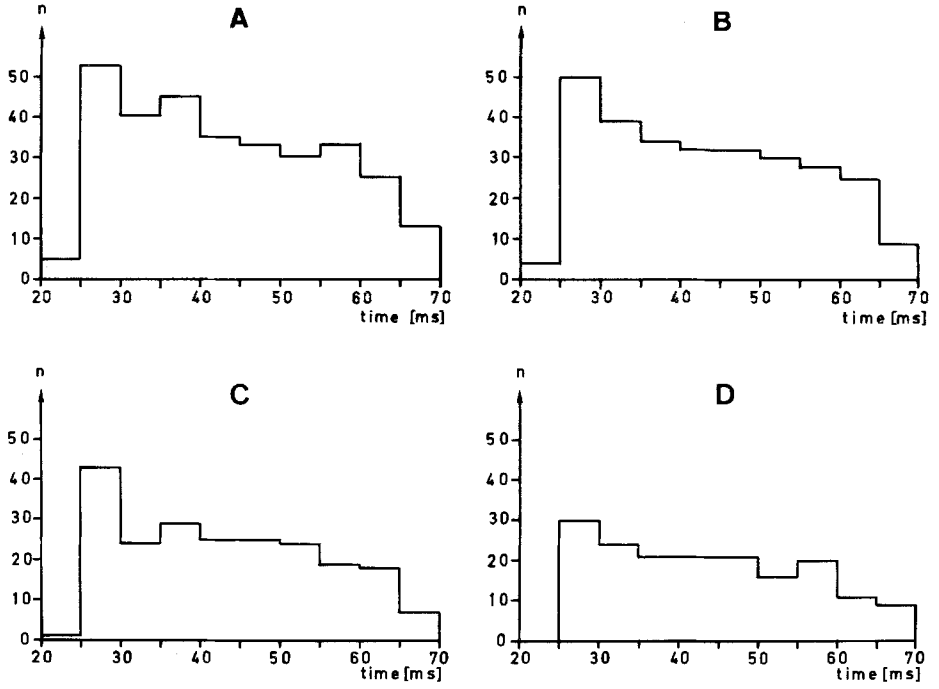

Fig. 16A–D. Post-stimulus time sequential histograms showing the spike responses of an omega cell (same cell as in Fig. 15) to excitatory stimuli presented at 65 dB. **A** No inhibitory stimulus. **B** Inhibitory stimulus set to 55 dB, **C** 65 dB, **D** 70 dB. *n* number of spikes per 5 ms summed over 30 sound pulses. Pulse duration: 50 ms, rise and fall times: 2 ms

connecting the main leg tracheae was cut on both sides of the septum. First the excitatory input (side ipsilateral to the cell body) was stimulated through cavity 2, and the intensity response of the omega cell was recorded. Then the sound pressure in this cavity was set to a constant level and the sound pressure level in cavity 1 (inhibitory input source) was varied. With increasing intensity to the inhibitory side, the response of the omega cell decreased almost linearly to 25% of the response in the absence of contralateral inhibition (Fig. 15B curve ●—●). Variation of the relative phase between sound signals in cavities 1 and 2 had no effect on the omega cell response, indicating a sufficient internal sound isolation after cutting the trachea.

If we assume bilateral symmetry for both omega cells and their presynaptic sensoric structures, we may determine the difference in spike activity between both omega cells for simultaneous stimulation of the two ears at slightly different sound pressure levels and compare this value with the difference in spike activity shown by the system when mutual inhibition is excluded. The ratio between these values then defines the gain of the omega-cell network due to mutual inhibition. For medium sound intensities (resultant sound pressure levels on both sides near 65 dB) a gain of about 1.6 can be deduced from the data in Fig. 15B (see Appendix B).

The latency of the omega-cell response with respect to the stimulus onset decreases with increasing excitatory intensity (Fig. 15B curve ○—○). For a constant ipsilateral intensity, the latency is not affected by a contralateral (inhibitory) stimulus which is less than or equal to the strength of ipsilateral

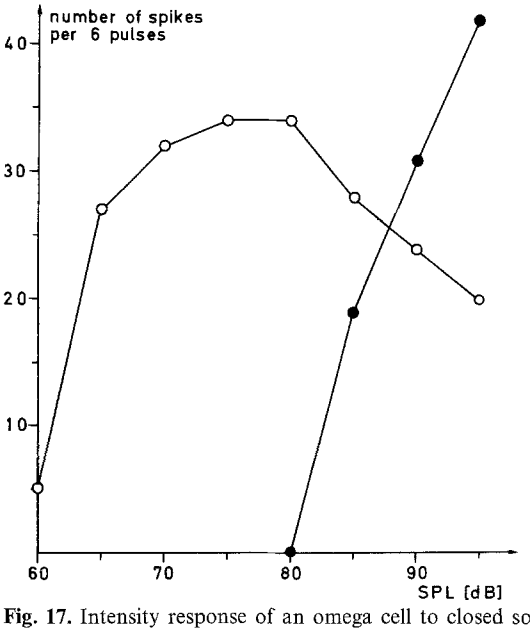

Fig. 17. Intensity response of an omega cell to closed sound field stimulation at 2 kHz with the contralateral leg nerve cut. Curve ○—○: response for ipsilateral sound presentation. Curve ●—●: response for contralateral sound presentation

(excitatory) stimulus. However, a contralateral stimulus of greater strength causes a slight increase in latency in addition to a reduction of spike number. The response latency of the complementary omega cell is now shorter than that of the recorded one. Therefore, inhibition affects even the beginning phase of the response in the recorded cell. This is illustrated by post-stimulus time sequential histograms for various stimulus situations in Fig. 16.

The contralateral inhibition is not the only inhibitory effect on the omega cell. At 2 kHz the intensity/response characteristic of the omega cell for ipsi- and contralateral stimulation reveals a second inhibitory mechanism. For ipsilateral stimulation (Fig. 17 curve o—o) the spike activity of the omega cell saturates between 70 and 80 dB. Above 80 dB the response decreases again. Contralateral stimulation via the tracheal system excites the omega cell to a much higher spike level than the saturation point from ipsilateral stimulation (Fig. 17 curve ●—●; note that the contralateral leg nerve was cut in this experiment). These effects are not present at frequencies above 2 kHz (cf. Fig. 8B).

Discussion

I. Closed Sound Field Stimulation with Condenser Microphones

The interpretation of neuronal responses to acoustic stimulation requires a knowledge of the stimulus parameters. Sound frequency and temporal pattern can easily be controlled when artificial sound signals are used. The effective stimulus intensity, however, is difficult to determine precisely in the complex four-input system of crickets.

In open sound fields stimulus strength is commonly defined by the dB-value of the sound pressure measured at the site of the tympanal membrane. The effective acoustic stimulus acting on each hearing organ is a result of both external *and* internal sound components and may differ considerably from the intensity of each component.

The closed sound field stimulation method separates the sound inputs such that single components can be applied independently. When presenting the external sound to both ears, the resultant sound pressure, which represents the effective stimulus acting upon each hearing organ, can be determined from the results of cancelling experiments (Fig. 11). The need of stimulus separation has been realized by several experimenters, and various attempts to solve the problem have been published. Lewis (1974a) and Nocke (1975) presented sound through small tubes; contact-mechanical vibration of tympanal membranes were reported by Lewis (1974b) and Rheinlaender and Mörchen (1979).

In crickets, closed sound chambers can easily be applied since the hearing organs are located in the frontlegs. The coupling of sound energy to the tympanal membranes is achieved through the air in the chambers and gives the same force distribution over the membranes as that produced under natural free-field conditions. The use of condenser microphones as sound transducers ensures excellent intensity and phase response of the system over a wide frequency range. These transducers can work in two different modes. In the absence of a polarization voltage a sinusoidal voltage of frequency f gives a sinusoidal sound output of frequency $2f$. This non-polarized frequency-doubling mode was used by Adams (1971) for stimulation of the acoustic receptor in the noctuid moth. In this case, all electronic components of the stimulus generator can be dimensioned to half of the acoustic frequency band used. But unfortunately, the square law of microphone membrane deflection, which is responsible for frequency doubling, generates a constant inwards deflection of the diaphragm as long as the alternating voltage is applied (see Frederiksen 1977). In a sound cavity this DC component of membrane motion causes a sudden pressure decrease. Because of small leaks in the system, the DC pressure component is gradually removed by the ambient air pressure. In our system the time constant τ of this process is in the order of the duration of a stimulus pulse; it gives rise to a strong distortion of the pulse envelope. τ can be shortened by enlarging the leaks, but this method destroys the good frequency response of the system.

Therefore, we chose to use a polarization voltage. But then the square law of membrane motion introduces intensity-dependent harmonic distortions limiting one to studies of auditory systems with very sharp frequency tuning (Schlegel 1977) such that higher harmonics lie outside the hearing range or to studies using low to moderate intensities (Adams 1971).

The hearing range of crickets, however, covers several octaves and a dynamic range of 35–100 dB SPL. This requires a low distortion factor in order to avoid unwanted two-tone stimulation. Appropriate electronic predistortion of the stimulus signal in a square rooter module solves the problem.

II. The Two-Input System

In *G. campestris* the attenuation of the tracheal pathway is rather high and thus the coupling between the two ears is weak. In the same species, Larsen and Michelsen (1978) measured the tympanal membrane vibration velocity in the two-input system and

found the internal sound pressure to be about 16–20% of the external one. This is equivalent to an attenuation Δ between 14 and 16 dB, and is similar to our results.

In *T. commodus*, Hill and Boyan (1977) found a threshold variation of approximately 16 dB in the two-input preparation when the direction of sound incidence was varied. Assuming a phase shift in the tracheal system that gives optimum destructive interference on the contralateral side, this is equivalent to an attenuation Δ in the tracheal pathway of 2.8 dB. This value contrasts with the measured tracheal attenuation in *G. campestris*. Further experiments have to be done to find out whether the discrepancy is caused by a species difference or if other factors such as age and history of the animals are responsible.

Assuming a species difference, we are left with the question of how *G. campestris* achieves effective directional hearing. In our closed sound field experiments we always found that the hearing system was very sensitive to external sound as long as the spiracles were open (rustling of paper induces a strong response in the omega cell). Thus we feel that the spiracular input is a very important factor in directional hearing. Here, the application of sound chambers is problematic as the surface structure of the cricket body in this region is complicated ad vibrational excitation of body tissue will likely occur. Preliminary experiments with a combination of closed and free-field stimulation show that cancelling can occur through the spiracles. Larsen and Michelsen (1978) demonstrated a strong influence of the spiracular input on the tympanal membrane vibration, but quantitative experiments involving the nervous system have yet to be performed.

III. The Coupling Process of Sound Energy to the Receptor Cells

In the cancelling experiments we assumed that the hearing organ is excited by the vibration of the large tympanum. Unfortunately, even the consistency of our experimental results does not prove this hypothesis. The tympanal membrane is not necessarily the origin of the resultant force driving the receptor cells. From the complex anatomy of the cricket hearing organ (Schwabe 1906; Michel 1974; Young and Ball 1974), speculations about the site of interaction between ipsilateral and contralateral sound components include principally two possible situations:

1. Ipsilateral and contralateral sound act on different sides of the same membrane (tympanum). Here both signals have to be in phase for destructive interference.

2. Ipsilateral and contralateral sound act on the same side of a membrane (a tracheal wall). Here both signals have to be 180° out of phase to obtain complete destructive interference.

In the first case one tympanal membrane, the toracic septum, and the tracheal tube contribute to the attenuation Δ and the phase shift φ of the tracheal pathway. In the second case both ipsilateral and contralateral sound components have to pass through a tympanal membrane. If we assume the cricket hearing system to be symmetrical in its biophysical properties, Δ and φ are not affected by the tympanal membrane, but they reflect the influence of the tracheal tube with its thin septum. Because of the different phase condition, 180° had to be added to the values of φ which have been measured in the cancelling experiments. For 5 kHz one would obtain $156° + 180° = 336°$, an unusually large phase shift for a short tube and a thin septum.

Recently, Fletcher and Thwaites (1979) calculated tympanal membrane displacement and tympanic sac pressure response for ipsilateral and contralateral stimulation using known and roughly estimated parameters of the auditory system of *T. commodus*. They found that contralateral sound always causes greater membrane displacement than ipsilateral sound. If the hearing organ were coupled to the membrane motion, contralateral sound would yield a stronger nervous response than isilateral sound; this is in contrast to the findings of Hill and Boyan (1977) in the same species. The calculated pressure response in the tympanal air sac, however, shows the ipsi/contra behavior required to explain the results of Hill and Boyan.

Cancelling experiments as described in this paper with simultaneous control of tympanal membrane vibration can reveal whether or not membrane motion is essential for excitation of the hearing organ. These experiments are in progress.

IV. Physiology of the Omega Cell

In order to characterize the omega cell morphologically and physiologically, properties of this acoustic intraganglionic interneuron have been studied (Casaday and Hoy 1977; Popov et al. 1978; Wohlers and Huber 1978). Both extra- and intracellular staining methods consistently yield a concrete morphological picture of the cell. Electrophysiological data reflect the neuronal context, the biophysical presensoric structure, and external field conditions. This has been shown for both the intensity response characteristics (Fig. 8 B) and for the frequency response of the omega cell (Fig. 14).

Under free-field stimulus conditions the iso-response and iso-intensity curves of the omega cell show characteristic oscillations with stimulus frequency (see Figs. 5 and 6 in Popov et al. 1978). Our closed-field threshold curve of the omega cell suggests that the

fine structure, if statistically significant, can partly be assigned to non-sensoric influences of the peripheral part of the hearing system and to external field conditions.

A further characteristic property of a neuron is its latency between stimulus onset and nervous response. In primary auditory fibers a linear relationship between latency and magnitude of nervous response (given as number of spikes per stimulus) has been found by Mörchen et al. (1978) and Esch et al. (1980). The latency measurement of the omega cell presented in this paper indicates that a simple linear correlation between response and latency, as found in the primary fibers, may not apply to higher-order neurons.

Quantitative analysis of contralateral inhibition reveals the omega cell to be more sensitive to one-sided excitatory stimulation than to contralateral intensity variation of the inhibitory input at constant excitatory sound input (compare the different slopes of the response curve ●——● in Fig. 15B). This would not be surprising in an unsymmetrical system. Recently, Wohlers (1980) showed by double-electrode recording, that when turning off one omega cell through hyperpolarization, the inhibitory effect of contralateral stimulation on the response of the complementary omega cell disappeared. Thus, each omega cell is excited by the primary acoustic fibers whereas the inhibitory influence has to pass through the complementary omega cell. If we assume bilateral symmetry of the excitatory pathway and suppose the inhibitory effect to be proportional to the current spike activity of the omega cell, the differences in sensitivity to ipsilateral stimulation on the one hand and combined ipsi/contra stimulation on the other hand may indicate that transfer of inhibition from one omega cell to the other is less effective than transfer of excitation from afferent fibers. The ipsilateral inhibition of the omega cell at 2 kHz, which is apparent from the intensity characteristics in Fig. 17, may result from excitation of a second modality. As the sound cavities enclose a short part of the cricket leg, low-frequency sound may cause vibrations exciting the subgenual organ. Afferent fibers of this sensorial structure arborize close to the input fields of the omega cell (Wohlers 1980). From the stainings of these neuropiles, a synaptic contact between the omega cell and afferents of the subgenual organ cannot be excluded.

Possible functions of the omega cells have been proposed earlier by Casaday and Hoy 1977; Hoy and Casaday 1978; Popov et al. 1978; Wiese 1978; Wohlers and Huber 1978. From our present analysis of contralateral inhibition we conclude that one functional aspect of the omega cell network is the enhancement of the contrast between ipsilateral and contralateral sound information (Wohlers and Huber 1978). Further conclusions can be made after simultaneously monitoring the activity of both omega cells and locating and characterizing the target cells.

We thank Prof. F. Huber and Prof. S. Penselin for their continued interest and helpful discussion, Peter Heinecke, Johannes Sagunsky, and Karl-Heinz Feist for building electronic equipment, and Franz Antoni for constructing the sound cavities.

Appendix A

The motion of tympanum T_2 (see Fig. 6A) produces the sound pressure p_2 in cavity 2. Tis amplitude $\hat{p}_2$ is given by:

$$\hat{p}_2 = \kappa \cdot \frac{p_-}{V_o} \cdot \Delta V \tag{1}$$

where $\kappa = \frac{c_p}{c_v} = 1.4$ the ratio of specific heats in air, $p_- = 10^5$ N/m^2 static air pressure, $V_o = 8.0 \cdot 10^{-8}$ m^3 cavity volume reduced for the volume of the inserted cricket leg, ΔV = peak volume reduction of the cavity volume caused by tympanal membrane oscillation.

We approximate the tympanal membrane T_2 by a rectangular membrane 1 mm × 0.3 mm in dimensions and assume parabolic displacement distribution (see Fig. 4 in Paton et al. 1977). Then the peak volume reduction ΔV is given by:

$$\Delta V \approx \frac{4}{9} \cdot \frac{A}{\omega} \cdot \hat{v} \tag{2}$$

where $A = 3 \cdot 10^{-7}$ m^2 the tympanal membrane area, $\hat{v}$ = velocity amplitude in the center of the membrane, ω = angular frequency.

Combining Eqs. (1) and (2), we obtain the center vibration velocity amplitude:

$$\hat{v} = \frac{9}{4} \cdot \frac{\omega V_o}{\kappa A p_-} \cdot \hat{p}_2. \tag{3}$$

Here $\hat{p}_2$ represents the sound pressure amplitude of the transmitted sound pressure in cavity 2 determined from the transmission curve ○——○ in Fig. 6B and extrapolated to a 100 dB level of the internal sound pressure p driving the tympanal membrane.

Appendix B

The two omega cells in the prothoracic ganglion will be labelled by a subscript $i = 1,2$ which refers to the sound chamber ipsilateral to the respective input side. From the rising part of curve ●——● in Fig. 15B we conclude that the response (spike number n_i) of an omega cell i is proportional to the suprathreshold excitatory stimulus $(L_i - L_t)$. Now we assume that the inhibiting effect of a given omega cell is proportional to the spike activity of the inhibiting cell. Thus:

$$n_1 = \alpha \cdot (L_1 - L_t) - \beta \cdot n_2, \tag{4}$$

and

$$n_2 = \alpha \cdot (L_2 - L_t) - \beta \cdot n_1. \tag{5}$$

In the absence of contralateral inhibition ($\beta = 0$) we obtain the spike activity difference between the two omega cells:

$$n_2 - n_1|_{\beta=0} = \alpha \cdot (L_2 - L_1). \tag{6}$$

With contralateral inhibition present ($\beta \neq 0$) the spike activity difference is given by

$$n_2 - n_1 = \frac{\alpha}{1-\beta} \cdot (L_2 - L_1). \quad (7)$$

Thus, gain g in spike number difference due to contralateral inhibition is determined by the ratio of Eqs. (7) and (6):

$$g = \frac{1}{1-\beta}. \quad (8)$$

To find β, we solve Eq. (4) and 15) with respect to the spike number n_2 of the recorded omega cell:

$$n_2 = -\frac{\alpha \cdot \beta}{1-\beta^2} \cdot L_1 + \frac{\alpha}{1-\beta^2} \cdot [L_2 + L_1(\beta - 1)]. \quad (9)$$

For a constant excitatory stimulus $L_2 = 65$ dB n_2 is proportional to the inhibitory stimulus L_1. From the falling part of curve ●——● in Fig. 15B we find the factor of proportionality $\alpha \cdot \beta/(1-\beta^2) = 5.1/20\ \mathrm{dB}^{-1}$. Inserting $\alpha = 12.5/20\ \mathrm{dB}^{-1}$ from the rising part of the same curve we find $\beta = 0.36$ and finally from Eq. (8) $g = 1.6$.

References

Adams WB (1971) Intensity characteristics of the noctuid acoustic receptor. J Gen Physiol 58:562–579

Boyan GS (1978) Coding of directional information by a descending interneuron in the auditory system of the cricket. Naturwissenschaften 65:212–213

Boyan GS (1979a) Directional responses to sound in the central nervous system of the cricket *Teleogryllus commodus* (Orthoptera: Gryllidae). I. Ascending interneurons. J Comp Physiol 130:137–150

Boyan GS (1979b) Directional responses to sound in the central nervous system of the cricket *Teleogryllus commodus* (Orthoptera: Gryllidae). II. A descending interneuron. J Comp Physiol 130:151–159

Casaday GB, Hoy RR (1977) Auditory interneurons in the cricket *Teleogryllus oceanicus:* physiological and anatomical properties. J Comp Physiol 121:1–13

Esch H, Huber F, Wohlers DW (1980) Primary auditory neurons in crickets: Physiology and central projections. J Comp Physiol 137:27–38

Fletcher NH, Thwaites S (1979) Acoustical analysis of the auditory system of the cricket *Teleogryllus commodus* (Walker). J Acoust Soc Am 66:350–357

Frederiksen E (1977) Condenser microphones used as sound sources. Brüel and Kjaer Technical Review No. 3

Hill KG, Boyan GS (1976) Directional hearing in crickets. Nature 262:390–391

Hill KG, Boyan GS (1977) Sensitivity to frequency and direction of sound in the auditory system of crickets (Gryllidae). J Comp Physiol 121:79–97

Hoy RR, Casaday GS (1978) Acoustic communication in crickets: Physiological analysis of auditory pathways. In: Burghardt G, Bekoff M (eds), Ontogeny of behavior. Garland Publ, New York, pp 45–62

Johnstone BM, Sounder JC, Johnstone JR (1970) Tympanic membrane response in the cricket. Nature 227:625–626

Kleindienst H-U (1978) Schallbeugung und -reflexion am Grillenkörper im Frequenzbereich 5–20 kHz. Verh Dtsch Zool Ges, 160

Kleindienst H-U (1980) Biophysikalische Untersuchungen am Gehörsystem von Feldgrillen. Dissertation, Rheinische Friedrich-Wilhelms-Universität Bonn

Larsen ON, Michelsen A (1978) Biophysics of the ensiferan ear III. The cricket ear as a four-input system. J Comp Physiol 123:217–227

Lewis DB (1974a) The physiology of the tettigoniid ear I. The implications of the anatomy of the ear to its function in sound reception. J Exp Biol 60:821–837

Lewis DB (1974b) The physiology of the tettigoniid ear II. The response characteristics of the ear to differential inputs: Lesion and blocking experiments. J Exp Biol 60:839–851

Michel K (1974) Das Tympanalorgan von *Gryllus bimaculatus* DeGeer (Saltatoria, Gryllidae). Z Morphol Tiere 77:285–315

Mörchen A, Rheinlaender J, Schwartzkopff J (1978) Latency shift in insect auditory nerve fibers. Naturwissenschaften 65:565

Nocke H (1974) The tympanal trachea as an integral part of the ear in *Acripeza reticulata* Guérin (Orthoptera, Tettigonioidea). Z Naturforsch 29c:652–654

Nocke H (1975) Physical and physiological properties of the tettigoniid ("grasshopper") ear. J Comp Physiol 100:25–57

Paton JA, Capranica RR, Dragsten PR, Webb WW (1977) Physical basis for auditory frequency analysis in field crickets (Gryllidae). J Comp Physiol 119:221–240

Popov AV, Markovich AM, Andjan AS (1978) Auditory interneurons in the prothoracic ganglion of the cricket, *Gryllus bimaculatus* DeGeer I. The large segmental auditory neuron (LSAN). J Comp Physiol 126:183–192

Rheinlaender J, Mörchen A (1979) "Time-intensity trading" in locust auditory interneurones. Nature 281:672–674

Schlegel P (1977) Calibrated earphones for the echolocating bat, *Rhinolophus ferrumequinum* . J Comp Physiol 118:353–356

Schwabe J (1906) Beiträge zur Morphologie und Histologie der tympanalen Sinnesapparate der Orthopteren. Zoologica 50:1–154

Wiese K (1978) Negative Rückkoppelung in der akustischen Bahn von *Gryllus bimaculatus* als Grundlage temporalen Filterns. Verh Dtsch Zool Ges 168

Wohlers DW (1980) Anatomical and physiological studies of the auditory pathway in crickets. Dissertation, Ludwig-Maximilians Universität München

Wohlers DW, Huber F (1978) Intracellular recording and staining of cricket auditory interneurons (*Gryllus campestris* L., *Gryllus bimaculatus* DeGeer). J Comp Physiol 127:11–28

Young D, Ball E (1974) Structure and development of the auditory system in the prothoracic leg of the cricket *Teleogryllus commodus* (Walker) I. Adult structure. Z Zellforsch 147:293–312

Zhantiev RD, Kalinkina IN, Tshukanov VS (1975a) The characteristics of the directional sensitivity of tympanal organs in *Gryllus bimaculatus* DeGeer (Orthoptera, Gryllidae). Entomol. Obozr. 54:249–256

Zhantiev RD, Kalinkina IN, Tshukanov VS (1975b) Functional characteristics of two auditory interneurons in the cricket *Gryllus bimaculatus* DeGeer (Orthoptera, Gryllidae). Vestn. MGU Ser Biol 6:18–25